El Cezeri
Journal of Science and Engineering
ISSN: 2148-3736

Research Article

Effect of Star Structure Versus Linear Polymers on Structure and Shear Rheology

Nese Cakir Yigit[1a]

[1]Department of Polymer Materials Engineering, Yalova University, Yalova, 77100, Türkiye
nese.cakir@yalova.edu.tr

DOI : 10.31202/ecjse.1735047
Received: 05.07.2025 Accepted: 30.09.2025
How to cite this article:
Nese Cakir Yigit, "Effect of Star Structure Versus Linear Polymers on Structure and Shear Rheology", El-Cezeri Journal of Science and Engineering, Vol: 12, Iss: 3, (2025), pp.(365-xx).
ORCID: [a]0000-0002-4714-4488

Abstract Star-shaped polymers have a compact molecular architecture and reduced entanglement density compared to linear analogues. They offer opportunities to tailor solutions and melt properties for various applications. This study examines the influence of polymer architecture on rheological behavior by comparing star-shaped polystyrene (PS) with linear PS. Star polymer was synthesized via atom transfer radical polymerization (ATRP) using a poly(divinylbenzene) (PDVB) core and PS arms. Both star and linear polymers with narrow molecular weight distributions were evaluated alongside a commercially available high-molecular-weight PS. Rheological measurements were performed at 25 °C in the presence of dioctyl adipate (DOA) plasticizer at varying shear rates. Under flow, polymer chains are dispersed, increasing free space and reducing molecular interactions. At higher shear rates, the polymers achieved the infinite shear viscosity plateau ($\eta\infty$). The commercially used linear PS mixture with DOA showed shear rate-independent behavior. Meanwhile, the star polymer had a smaller hydrodynamic volume and gyration radius, resulting in lower viscosity.

Keywords: Linear polymer, Multiarm star polymer, Polymer characterization, Rheology.

I. INTRODUCTION

Star polymers, characterized by multiple arms extending from a central core, represent a class of branched macromolecules with a compact structure, globular shape, and extensive surface area. Incorporating diverse functional groups into star polymers significantly broadens their potential applications, including polymer therapeutics, diagnosis, optical imaging, membranes, coatings, viscosity modifiers, catalysis, separation media, thin films, and numerous other advanced materials [1-3].

Atom transfer radical polymerization (ATRP) is among the most widely used living polymerization techniques for synthesizing star polymers. Two primary synthetic strategies are employed: "core-first" and "arm-first" approaches [4-6]. In the "arm-first" procedure, the addition of the cross-linker at a specific conversion of the monomers occurs in a "one-pot" process. A "two-pot" process conducts the synthesis of star polymers using the purified linear polymers, known as macroinitiators (MIs). These techniques effectively synthesize numerous monomers into star-like polymers, such as methyl methacrylate, styrene, and tert-butyl acrylate. Despite polymerization using "core-first" and "arm-first" methods, all the arms of these star polymers display linear characteristics [7-10].

Linear polymers generally exhibit poor mechanical properties and limited thermal stability; therefore, cross-linking reactions, such as those applied in the construction of star polymers, are commonly employed to generate polymer networks with enhanced elasticity, thermal resistance, and porosity. Additionally, star polymers possess compact structures with reduced entanglement, abundant functional groups, and superior processability. These characteristics define their unique physicochemical properties, including lower glass transition temperatures, reduced bulk and solution viscosities, increased solubility, and enhanced ease of processing and modifications. Star polymers, in particular, have attracted growing interest in gene delivery and nanomedicine, as their unique architecture enables the encapsulation of genetic material within their cores, thereby allowing efficient regulation of gene release into the cytosol. Consequently, star polymers have garnered considerable attention in recent years and are increasingly recognized as promising materials for a wide spectrum of technological and biomedical applications [3, 11-13].

A rheological study ranges from viscoelastic liquids to viscoelastic solids for analyzing Newtonian or non-Newtonian fluids, examining shear rate and shear stress, thereby providing valuable insights into their intrinsic fluid properties [14, 15]. The characteristics of the rheological properties of star-shaped systems are influenced by the dynamics of two components: the linear arms and the core, which move in conjunction with the arms. As a result, star polymers with a low number of arms *f* have a Gaussian coil conformation; stress relaxation is independent. As the *f* in the star polymer increases, the compression of the structure leads to a further decrease in the viscosity of the samples. High *f* values and significant core size lead to a core-shell structure, requiring rheological behavior analysis concerning the compact centers of star macromolecules [16-18]. Moreover, computer simulations demonstrated that the behavior of multiarm star-shaped polymers in suitable solvents resembles that of solid particles and markedly differs from that of classical coil-like macromolecules [19].

Liu et al. investigated the effect of short arms on the rheological behavior of star polymers. Their study showed that as the short arm length increases, the linear viscoelastic rubber plateau decreases, which causes the relaxed short arms to act as a "solvent" and dilute the polymers. They found their work encouraging for guidance on molecular design to tune linear and nonlinear rheology in star polymers [20]. Van Ruymbeke et al. investigated a quantitative assessment of star rheology using a simple model accounting for high-frequency response and low-frequency arm relaxation. They observed deviations and confirmed the universal mechanism of arm relaxation governing star rheology. However, they mentioned that subtle issues must be addressed for accurate quantitative dynamics [21].

Although star-shaped polymers have been extensively studied in academic research, their industrial application remains limited. Key challenges include reducing preparation costs and simplifying synthetic routes and purification processes, particularly for removing linear or star-star coupled products, toxic metal catalysts, and odorous compounds. Addressing these issues is essential for broader industrial adoption of star polymers [22]. Mandal et al. synthesized narrowly dispersed and degradable homoarm and miktoarm star polymers in one pot using the catalytic living ring-opening metathesis polymerization (ROMP) mechanism with vinyl ether chain transfer agents. They argued that this sustainable and environmentally friendly method offers a valuable synthetic tool for polymer engineers in supramolecular, industrial, or biomedical research [23]. Sparnacci et al. investigated a synthetic procedure for core-crosslinked star copolymers suitable for direct industrial implementation. Using the arm-first technique, they synthesized core-cross-linked star (CCS) copolymers via reversible addition-fragmentation chain transfer polymerization (RAFT). They evaluated their performance as viscosity index improvers in hydraulic lubricants. For comparison, a commercial linear PMA-type transmission oil was also tested. The study demonstrates that by adjusting the properties of CCS polymers, these materials can serve as model lubricant formulations for hydraulic applications and fluid production [24].

Moreover, star polymers have been successfully applied in the coating industry as rheological regulators, enhancing material processing and liquidity. Studies on drilling fluid systems based on star polymers have appeared in some papers in recent years. Luo et al. published an acrylamide-based star-shaped copolymer for water-based drilling fluids with better rheological properties and more effective filtration performance at high temperatures that can address the limitations of linear polymeric additives [25]. Jian et al. recently developed a new generation of amphoteric star polymers, which exhibited high molecular weight, branching density, and surface area for drilling fluid systems. The polymer formed aggregates, generated stable emulsions in the study, and maintained plastic viscosity under high-temperature conditions. The star polymer produced thin filter cakes and minimal fluid loss volume in oil-based mud systems, demonstrating excellent fluid control and rheology profiles [26].

Herein, in two steps, we used an “arm-first” strategy to produce a multi-arm star PS of absolute molecular weight using atom transfer radical polymerization (ATRP). We also investigated the nonlinear rheological behavior of multiarm star PS chains and compared the results with the behavior of linear PS polymers with approximately the same molecular weights. Furthermore, all synthesized star and linear polymers were compared with the commercially available PS polymer for rheological properties to see the effect of precise molecular weight control and narrow molecular weight distribution on the architecture.

II. EXPERIMENTAL SECTION

2.1 Materials

Styrene (St, 99% Aldrich) and divinyl benzene (DVB, 80%, Aldrich) were purified by passing through a column filled with basic alumina to remove the inhibitor immediately before use. N, N, N′, N″, N″-Pentamethyldiethylenetriamine (PMDETA, Aldrich) was distilled over NaOH before use. Ethyl α-bromoisobutyrate (EiBr, 98%), CuBr (99.9%), and all solvents were purchased from Aldrich and used as received. PS average M_w ~192,000 was provided by Aldrich and used as received. Polyethylene glycol 400 (PEG) was purchased from Ataman Chemicals (Türkiye). The plasticizers dioctyl terephthalate (DOTP), epoxidized soybean (ESBO), and dioctyl adipate (DOA), all with 99% purity, were obtained from Plastay Chemistry (Türkiye).

2.2 Characterization

Polymers were characterized by gel permeation chromatography (GPC). The GPC measurements were carried out with an Omnisec multi-detector GPC instrument from Malvern Panalytical Ltd. (Worcestershire, U.K.) equipped with four-column PL gel 5 mm Mixed-C and multi-detector including refractive index, UV/visible PDA, viscosimetric, and light scattering detectors to measure the molecular weight distribution and absolute molecular weights of polymers in tetrahydrofurane (THF) as a mobile phase calibrated with a narrow molecular weight distributed PS standard. The flow rate of THF was 0.9 mL/min at 35 ^{o}C. The concentrations of sample solutions were prepared as 1 to 5 mg/mL, and the injection volume was 0.1 mL. A differential refractive index (dn/dc) of 0.185 mL/g was measured for PS.

The Agilent 6890N gas chromatograph (GC), equipped with a 7683 automatic liquid injector, an FID detector, and a 3-meter 180-µm DB-1 capillary column, followed the star formation. The injector and detector temperatures were maintained at 280

°C and 285 °C, respectively. The initial column temperature is 40 ºC, ultimately increasing to 120 ºC at a heating rate of 40 ºC/min.

Fourier transform infrared (FTIR) spectroscopy measurements (FTIR) were obtained using an Agilent Technologies Cary 630 FTIR instrument within the 4000–500 cm^{-1} range.

The hydrodynamic diameters of the polymers were determined using dynamic light scattering (DLS) using a Malvern NanoZSP instrument with a He-Ne laser operating with a 632 nm wavelength at an angle of 173 ºC. Samples were prepared at a 1 mg/mL concentration in THF dispersions.

Differential scanning calorimetry (DSC) was conducted using a TA Instruments Q2000 Series Thermal Analysis System equipped with an autosampler within a temperature range of −80 to 400 °C at a 10 °C min-1 heating rate under a nitrogen atmosphere and using approximately 5 mg of sample.

Rheological measurements were conducted using the TA Instruments Discovery Hybrid Rheometer HR-2, equipped with a 220 mm holder and a parallel steel plate. All measurements were recorded at 25 ± 0.01 ºC.

2.3 Synthesis of linear polymers by ATRP

Linear polystyrene (PS) polymers (P1 and P2) were prepared by ATRP of St using PMDETA ligand and a copper(I) catalyst. Two different monomer: initiator ratios were used: [M]/[I] = 200 for P1 and [M]/[I] = 2000 for P2, with EiBr as initiator. A typical experimental procedure is as follows: St (P1 = 20.0 mL, 175.0 mmol; P2 = 50.0 mL, 436.0 mmol), PMDETA (P1 = 0.183 mL, 0.875 mmol; P2 = 0.045 mL, 0.218 mmol), CuBr (P1 = 0.125 g, 0.875 mmol; P2 = 0.031 g, 0.218 mmol), and EiBr (P1 = 0.128 mL, 0.875 mmol; P2 = 0.032 mL, 0.218 mmol) were added in sequence to a Schlenk flask with a magnetic stirring bar. The flask was sealed with septa. Then the reaction mixture was degassed by three freeze–pump–thaw cycles. After degassing, the Schlenk flask was left in a vacuum and placed in a thermostated oil bath at 110 ºC. Following a 45-minute polymerization of P1 and a 24-hour polymerization of P2, the flask was cooled to room temperature and exposed to oxygen to terminate the polymerization. Subsequently, the polymerization mixture was diluted with THF, passed through a basic alumina column to remove the catalyst, and precipitated in excess methanol. The polymer was dried for 24 h in a vacuum oven at 40 °C (P1 = 5.6 g, 31% yield, P2 = 15.5 g, 34% yield).

2.4 Synthesis of multiarm star polymer by "arm-first" technique

P1 (2.0 g, 0.267 mmol) was dissolved in 11 mL of anisole in a Schlenk flask equipped with a magnetic stir bar, achieving a total macromonomer concentration of 0.023 M in the reaction. DVB (0.570 mL, 4.01 mmol), PMDETA (0.056 mL, 0.267 mmol), and CuBr (0.038 g, 0.267 mmol) were added to the solution. After dissolution, an aliquot (~ 10 mL) was quickly removed from the reaction mixture for GC analysis. The mixture in the Schlenk flask was degassed by three freeze–vacuum–thaw cycles. Then, filled with argon gas, sealed, and immersed in a thermostated oil bath at 110 ºC. Samples were taken from the reaction mixture periodically to screen DVB conversion. After 24 h at 95 % conversion, the reaction was stopped, diluted in THF, and passed through an alumina column. The entire reaction mixture was dried on a rotary evaporator, redissolved in CHCl3, and precipitated in a methanol/diethyl ether (1/3; v/v) mixture, recovered by suction filtration, and dried in a vacuum oven at 40 ºC for overnight.

III. RESULTS AND DISCUSSION

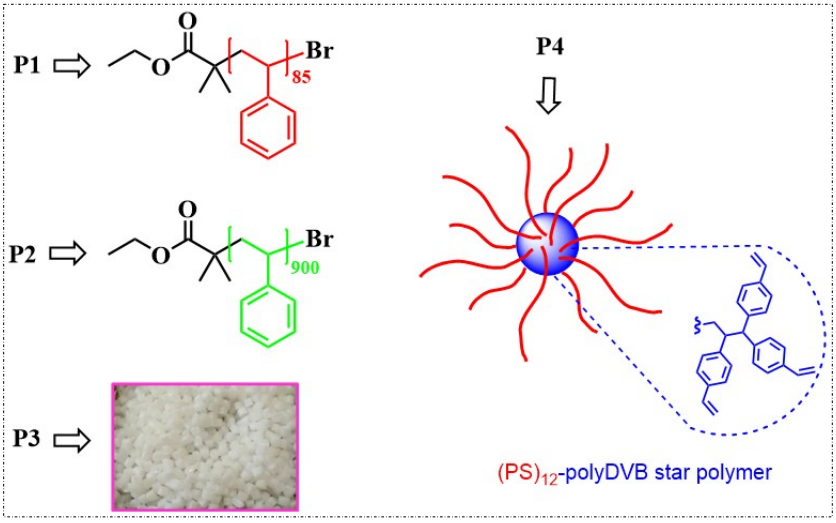
The present study involves the rheological comparison of the synthesized low and high-molecular-weight linear PS polymers, a multiarm star PS polymer consisting of PDVB core and short PS homopolymer arms, and commercially available linear PS with high molecular weight distribution. Scheme 1 illustrates all the P1-P4 polymers investigated in this study.

First of all, we employed the ATRP reaction of styrene monomer to obtain linear low-dispersity PS samples using EiBr as an initiator and CuBr/ PMDETA as a catalyst in bulk polymerization at 110 ºC, as described earlier [27]. Linear polymers possessing 2-bromoisobutyryl end-groups were synthesized with narrow dispersity values using a feed ratio of St: EiBr/200:1 and 2000:1 for P1 and P2, respectively. The initiating end group: catalyst: PMDETA ratio was 1:1:1 in all cases. The polymers were purified by passing their solution in THF through a column filled with neutral aluminum oxide, followed by evaporation of the solvent and precipitation into methanol. Results of molecular weight values (M_n and M_w) and dispersity (PDI) are depicted in Table 1.

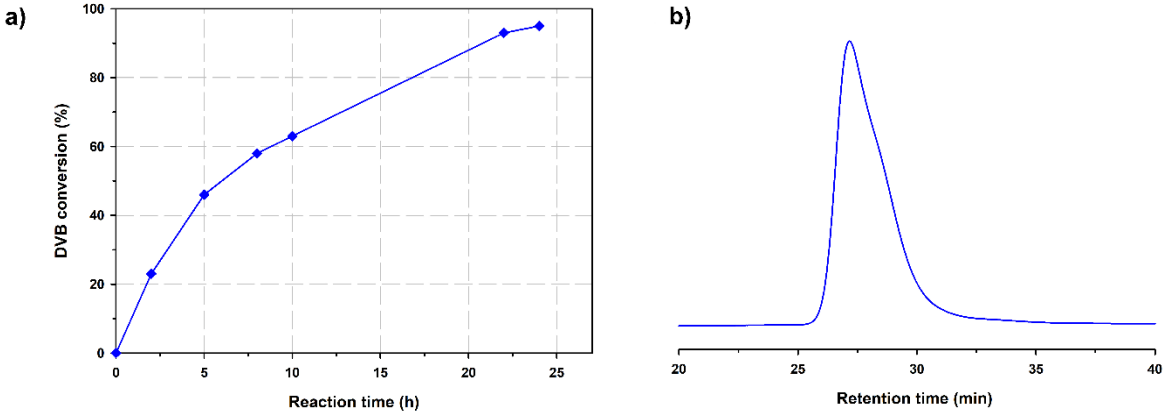
In addition to these synthesized polymers, high molecular weight PS (P3) was purchased commercially from Aldrich to see whether the rheological properties of linear or star polymers with narrow molecular weights were superior to broad distribution polymers. The molecular weight values, polydispersities, and intrinsic viscosities of all polymers for which rheology measurements were made are shown in Table 1.

Multiarm star polymer (P4) was prepared by ATRP, and the “arm-first” method using P1 as a macroinitiator. The P1 was crosslinked with DVB to form a multiarm $(PS)_n$-polyDVB star polymer (P4). The star formation was monitored by the GC instrument. The samples were diluted with $CHCl_3$ to an appropriate concentration for the GC. The time-dependent conversion of DVB was calculated from the ratio of the peak area of DVB to the peak area of the internal standard anisole. Until 50% DVB conversion, the plot in Figure 1a was linear. The curvature at higher DVB conversion may have been caused by certain

alkyl bromide initiating sites within the highly cross-linked polyDVB core becoming less accessible and less likely to be activated and react with DVB. After 24 hours, the reaction was stopped at 95% DVB conversion, and the mixture was purified by fractional precipitation from THF into a methanol/diethyl ether mixture to eliminate unconverted linear PS. Figure 1b shows the relevant GPC chromatogram of the purified multiarm star polymer with monomodal distribution. As envisaged, PS homopolymer was used as a macroinitiator for synthesizing a multiarm star polymer, and subsequent purification steps were effectively carried out.



(1)



(2)

Figure 1. (1) Structures of star and linear polymers used in this study. Low molecular weight linear PS (P1) is highlighted in red, high molecular weight linear PS (P2) is highlighted in green, and commercially obtained high molecular weight linear PS (P3) is framed in pink. The DVB core of multiarm star polymer (P4) is highlighted in blue with linear red arms (P1). (2)a) Kinetic diagram of the DVB conversion, obtained via GC, depending on the star polymer synthesis reaction time. b) Corresponding RI-trace of purified multiarm $(PS)_n$-polyDVB star polymer (P4), obtained via GPC in THF at 35 ºC.

All of the obtained polymers, P1-P4, exhibited monomodal GPC traces, as shown in Figure 2a. The commercially available P3 polymer had a relatively broader molecular mass distribution than the ATRP systems used in synthesizing other polymers (P1, P2, and P4), indicating that an uncontrolled polymerization was used.

Figure 2b shows the FTIR spectra of all polymers, P1-P4. The C–H aromatic stretching vibrations were observed at 3060 and 3025 cm^{-1}, while the C–H stretching vibration occurred at 2925 cm^{-1}. Additionally, the phenyl ring stretching vibrations were noted at 1600, 1496, 1460, 750, and 700 cm^{-1}, indicating the presence of typical absorption bands for PS across all polymers. As all the polymers (P1-P4) bear structural similarities, they showed similar spectral properties. Moreover, due to the appearance of the intense characteristic bands of PS arms, star polymer (P4) showed similar bands to its homopolymer (P1) signals.

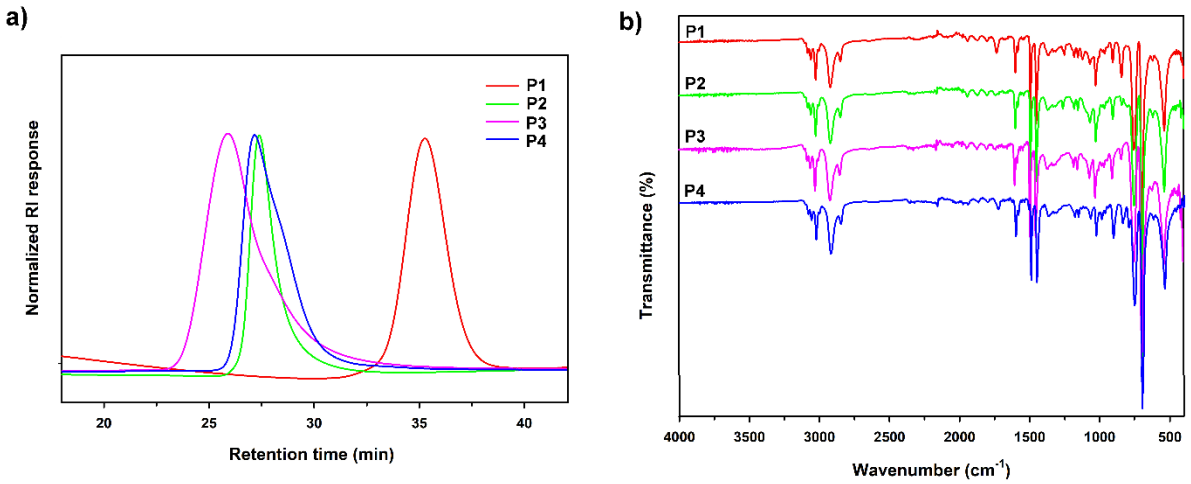


Figure 2. a) GPC chromatograms of all P1-P4, in THF at 35 °C. b) FTIR spectrum of all polymers, P1-P4.

Table 1 shows the actual molecular weight (M_w = 129000) of $(PS)_n$-polyDVB multiarm star polymer obtained by multi-detector GPC, with the introduction of the d*n*/d*c* = 0.185 mL/g of linear PS standard. Since the star polymer was obtained by the "arm first" technique, the average number of arms *f* per star macromolecule was calculated by using the molecular weight of the entire star together with the weight of the macroinitiator (MI) under the assumption that the crosslinking agent used was incorporated into the polymer core, with the following equation (1):

$$f = \frac{M_{w,star}}{M_{w,arm} + [DVB]/[PS]\ x\ M_{DVB}\ x\ conv_{DVB}} \quad (1)$$

Here, $M_{w,star}$, $M_{w,arm}$ are the weight-average molecular weights of the star polymer and macroinitiator, respectively, and [DVB]/[PS], M_{DVB}, $conv_{DVB}$ are the feed molar ratio of the crosslinker to macroinitiator, the molecular weight, and conversion of crosslinker. As given in Table 1, *f* was calculated to be 12 using equation (1).

The intrinsic viscosities ([η]) of all polymers, P1-P4, were determined by multi-detector GPC in THF at 35 °C, as shown in Table 1. For polymers P1, P2, and P3, [η] increased with molecular weight. A low viscosity value was measured for the star polymer, P4. As expected, star polymers have a compact structure, which leads to a decrease in the viscosity of the samples. Moreover, with the increase in the number of arms, a further compaction of the structure and a further reduction in the viscosity of the samples are observed [28]. It is generally recognized that the most expedient technique for elucidating the structure of star polymers is to compare the intrinsic viscosity of the star polymer $[\eta]_{star}$ and its linear analog with the same molecular weight, $[\eta]_{linear}$, where g' is the contraction factor, as given in equation (2) [29].

$$g' = [\eta]_{star} / [\eta]_{linear} \quad (M = \text{constant}) \quad (2)$$

The intrinsic viscosity for linear PS, $[\eta]_{linear}$ with comparative molecular weight was obtained from the Mark–Houwink–Sakurada (MHS) equation, as given in equation 3. The MHS values of K = 1.44 x 10^{-4} dL/g and α = 0.707 were obtained from the literature for linear narrow PS in THF at 35 °C [8]. Then, using these parameters $[\eta]_{linear}$ was calculated to be 0.59 dL/g for a specified molecular weight (M_w = 129000 g/mol) of linear PS. Moreover, the $[\eta]_{star}$ of star polymer was measured to be 0.174 dL/g by the viscometer detector in multi-detector GPC.

$$[\eta] = K\ x\ M^{\alpha} \quad (3)$$

It is also demonstrated that the number of arms, *f*, is inversely proportional to g' in regular star polymers with equal arm lengths, as shown in equation 4. Then, *f* was calculated as 13, which closely agrees with the result obtained from equation 1.

$$\log g' = 0.36 - 0.8 \log f \quad (4)$$

Table 1 also shows the hydrodynamic radius (R_h) of all polymers, P1-P4. As expected, the increased molecular weights increased the R_h values of polymers.

Table 1. Multi-detector GPC data of polymers P1-P4

Polymer	Architecture	f^e	M_n (g/mol)	M_w (g/mol)	*PDI*	[η] (dL/g)	R_h (nm)
P1	Linear [a]	-	7500	8800	1.17	0.082	2.19
P2	Linear [b]	-	80000	94000	1.17	0.46	6.72
P3	Linear [c]	-	104100	198000	1.91	0.73	9.23
P4	Star [d]	12(13) [f]	98500	129000	1.31	0.174	7.51

[a] $[M]_0$:$[I]_0$:[CuBr]:[PMDETA] = 200:1:1:1; ATRP reaction at 110 °C for 45 min.
[b] $[M]_0$:$[I]_0$:[CuBr]:[PMDETA] = 2000:1:1:1; ATRP reaction at 110 °C for 24 h.
[c] Obtained commercially from Aldrich.
[d] $[DVB]_0/15 = [P1]_0 = [CuBr]_0 = [PMDETA]_0$= 0.023 M in anisole at 110 °C for 24.
[e] Calculated according to equation (1).
[f] Calculated according to equations (2), (3), and (4).

Particle size measurements were established for P1-P4 in THF suspension by DLS. Figure 3 revealed that DLS data weighted by numbers (Figure 3a) and volume (Figure 3b) of P1-P4 obtained. The number-weighted DLS measurement of the samples and the volume-weighted exhibited one peak with unimodal particle size distributions for all samples analyzed. The hydrodynamic diameter (D_h) value indicated an increase from 3.73 nm to 10.82 nm (number-average) after crosslinking the linear polymer (P1) to form the star polymer (P4). Comparing the D_h values of linear PS polymers, P1-P3, there was a linear relationship between the intensity of the light scattered and the increase in molecular weight, resulting in a larger size.

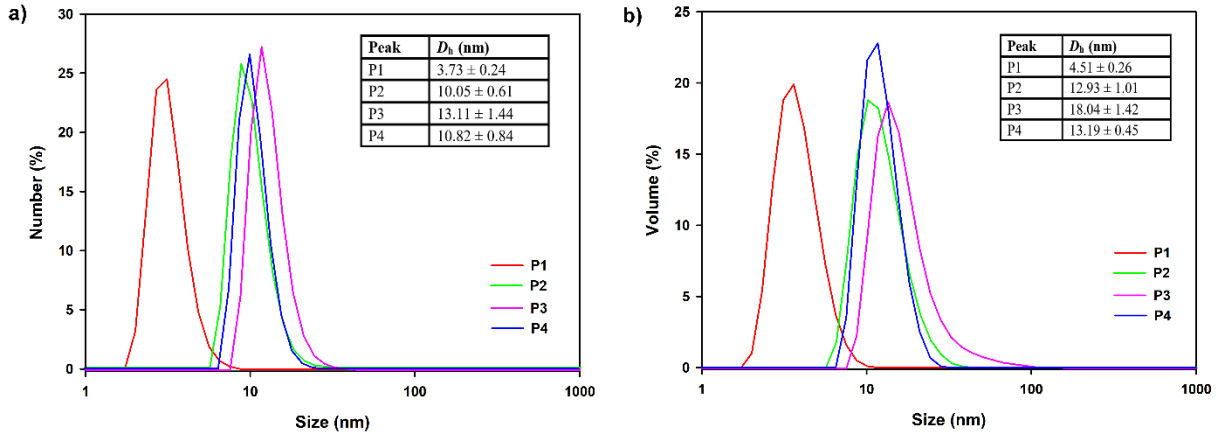


Figure 3. Dynamic light scattering (DLS) measurements of the size dispersion of P1-P4 samples represent data weighted by number (a) and volume (b) of particles.

The thermal behaviour of polymers, P1-P4, was studied by DSC. As shown in Figure 4a, DSC measurements showed the glass transition temperatures (T_g) of P1-P4 to be 95.6 °C, 108.1 °C, 103.8 °C, and 105 °C, respectively. Generally, the T_g of polymers was shifted to higher temperatures (from 95 to 105 °C) with increased molecular weights. As expected, no crystalline fraction was observed in all the polymers. For the multiarm star polymer (P4), broad glass transitions were observed by DSC. Interestingly, the T_g of the PS arm cannot be detected. This can be due to its partial miscibility with the polyDVB core, which may lead to a plasticizing effect and thus significant broadening of the T_g of the star polymer. In addition, the unique structure of star-shaped copolymers hinders the movement of segments.

As shown in Figure 4b, the crystallization peak of the PS segments was evident for all polymers. Moreover, the crystallization peak of PS in the multiarm star polymer (P4) was more prominent. This can be because the PS chains are directly connected to the star core molecule and give better mobility to the PS chains, which is advantageous for crystallization.

For rheological measurements, the miscibility of the four most commonly used plasticizers with PS was tested by selecting the P3 polymer as a reference. P3 polymer solutions containing different plasticizers were prepared at a concentration of 20% w/w. Concentration was calculated as c(% w/w) = (m_{PS}/(m_{PS}+ $m_{plasticizer}$)) x 100. Chloroform ($CHCl_3$) was chosen as a cosolvent; P3 was dissolved in $CHCl_3$, and plasticizers were added to the polymer solutions individually. After that, $CHCl_3$ was evaporated during stirring under ambient conditions for up to 2 days until the sample weight stabilized. As depicted in Figure 5, phase separation occurred in PS polymer blends containing PEG, DOTP, or ESBO after solvent evaporation.

However, the PS mixture containing DOA was transparent and viscous, so we used the DOA-containing P1, P2, P3, and P4 blends.

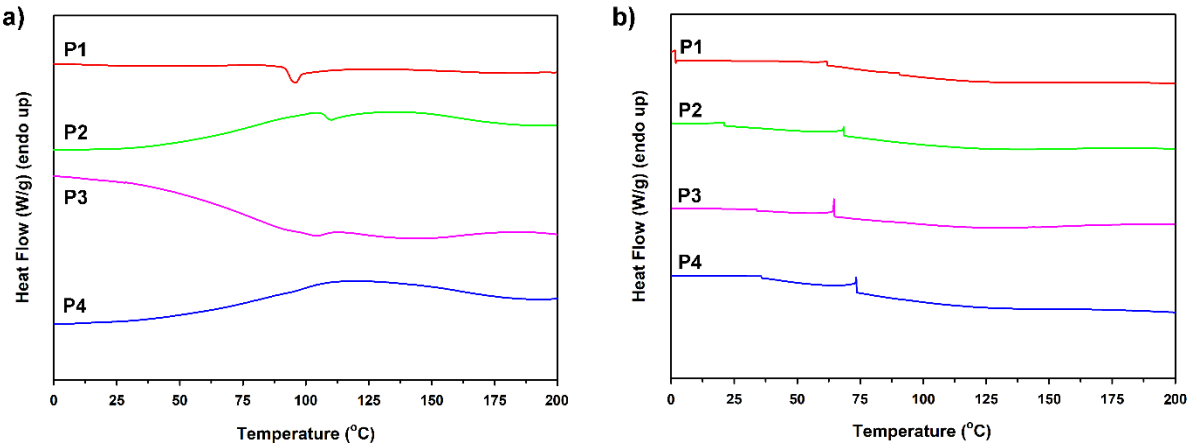


Figure 4. DSC curves for polymers P1- P4 with scanning rates of 10 °C min^{-1} (a) first heating run and (b) first cooling run.

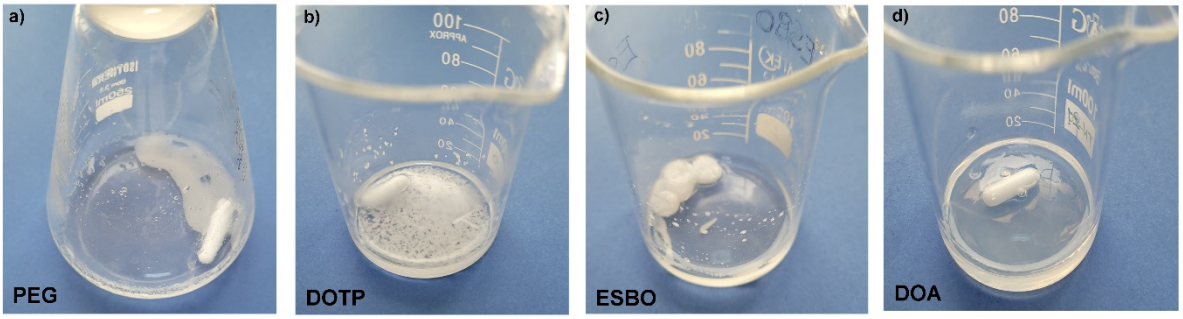


Figure 5. Images of blends containing P3 with (a) PEG, (b) DOTP, (c)ESBO, and (d) DOA

A parallel steel plate performed rheological measurements. Since the samples are PS blends containing plasticizers, parallel plate measurements are more suitable for this high-viscosity sample, as they provide good contact between the rheometer plate surfaces and the polymeric liquid. Slip is also prevalent when employing rheometers to test highly concentrated polymer solutions. The measured viscosity can be substantially lower than the actual viscosity of the sample when leakage occurs. To address these limitations, slip tests were conducted on samples with varying gap heights and geometries. It was determined that slip was not occurring within the measured range of shear and strain.

A shear rate sweep test ranging from 10^{-2} to 10^{3} s^{-1} was performed to examine the rheological properties of the polymer solutions. Figure 6 illustrates the flow curves for all DOA-containing PS samples at a concentration of 20% w/w (P1-P4 blends). Polymers in solution showed a shear rate-dependent viscosity behavior below a critical shear rate γ_{crit}, termed the non-Newtonian power-law region, where the viscosity decreases as the shear rate increases. One possible explanation for the relation between shear rate and viscosity is that molecular alignment under shear facilitates the flow of polymer chains, reducing shear viscosity as the shear rate increases. The other observation was the relation between molecular weight and viscosity. The dependence of viscosity on shear rate is initiated at lower γ levels with an increase in molecular weight. Above this γ_{crit}, the solution viscosity remained constant regardless of shear rate, referred to as the zero-shear viscosity, η_0. The transition from shear-rate-dependent to shear-rate-independent viscosity occurred within a comparatively narrow region due to the P1, P2, and P4 samples with a narrow molecular weight distribution. Additionally, Figure 6a indicates that assessing molecular weight degradation caused by shear forces presents challenges in the non-Newtonian region, as samples with varying molar masses exhibit constant viscosity at a specific shear rate. DOA-containing P3 blends showed totally shear-rate independent behavior because they are commercially available with high PDI.

Figure 6b presents the shear stress versus the shear rate flow curves of P1-P4 blends. All samples exhibited shear-thinning behaviour, particularly in lower molecular weight PS blends.

The viscosity of the samples decreased with increasing shear rate and exhibited an infinite shear viscosity (η_∞) at high shear rates. The flow behavior of all samples demonstrated shear-thinning Non-Newtonian characteristics, which intensified with the increasing molecular weight of PS in the DOA-containing PS samples, ultimately transitioning to a more Newtonian behavior.

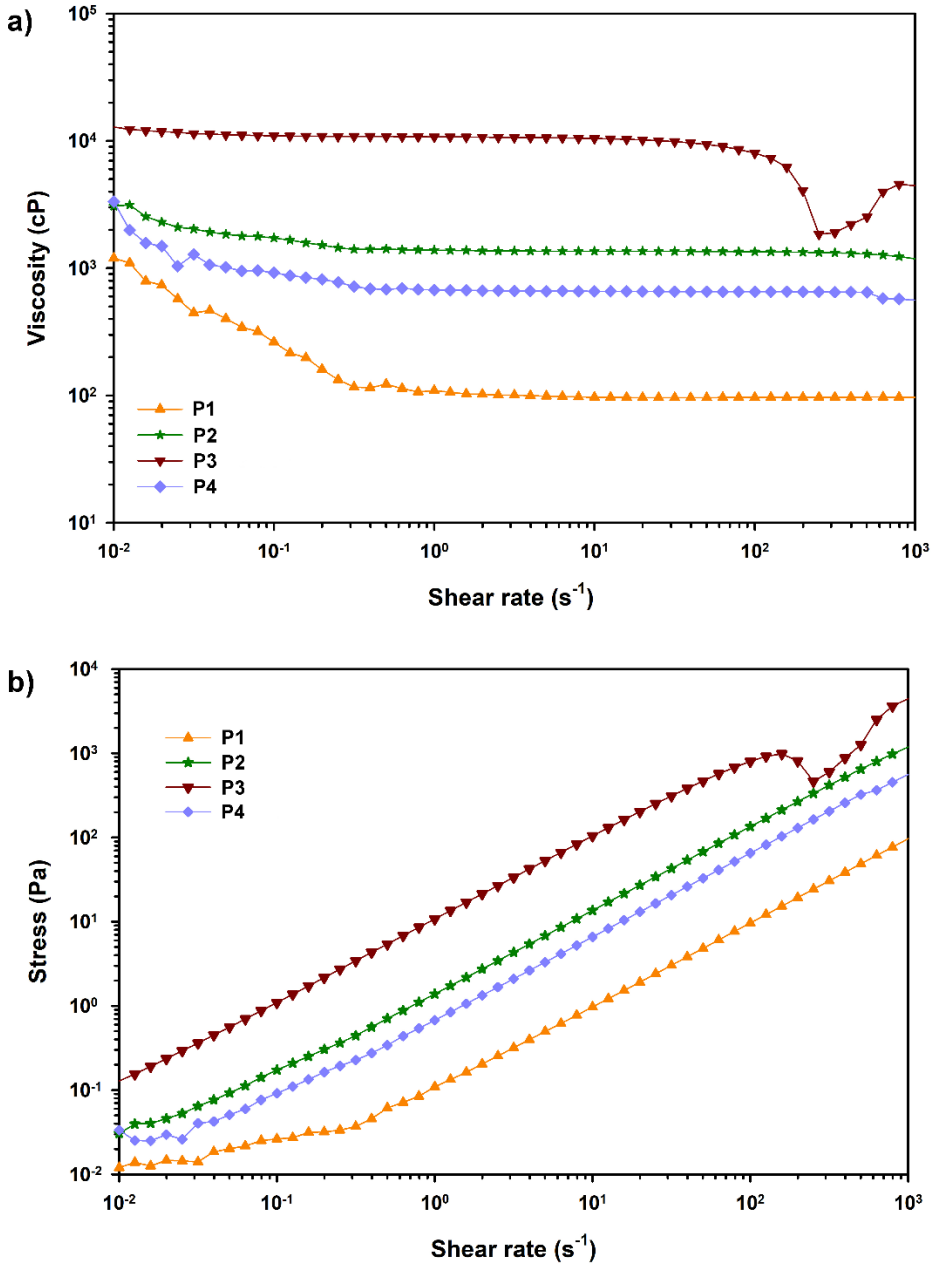


Figure 6. a) Dependency of the shear viscosity on the shear rate for P1-P4 samples, b) Shear stress versus shear rate for P1-P4 samples at 25 °C.

Table 2. Zero-rate and infinite-rate viscosities and coefficient values fitting with Carreau and Cross Models

Samples	η_0 (mPa.s) Zero-Rate Viscosity	η_∞ (mPa.s) Infinite-Rate Viscosity	R^2 Carreau Model	R^2 Cross Model
DOA only	499.511	13.7095	0.9832	0.9832
P1:DOA	1240.35	97.0102	0.9931	0.9939
P2:DOA	3070.90	1334.02	0.9830	0.9830
P3:DOA	10283.4	2686.23	0.9021	0.9001
P4:DOA	3258.37	570.746	0.8599	0.9253

Furthermore, an increase in the molecular weight of PS resulted in a slight increase in the parameter η_∞, indicating a rise in viscosity, as demonstrated in Table 2. The Carreau and Cross model was employed regarding the overall error in estimates of the non-Newtonian viscosity-shear rate relationship, and the results indicated a comparable shear-thinning flow behavior.

IV. CONCLUSIONS

This study reports how variations in polymer architecture affect rheological properties by systematically comparing star-shaped polystyrene (PS) to its linear counterparts of similar molecular weight and to high-molecular-weight, broad-distribution linear PS. Research begins with synthesizing a star-shaped polymer with a poly(divinylbenzene) (PDVB) core and PS arms using ATRP polymerization. This star-branched PS displays relatively narrow molecular weight distributions due to well-ordered arms. Linear PS samples with approximately the same molecular weight are prepared by conventional ATRP to compare the effects of architecture on rheology directly. Additionally, high-molecular-weight PS with a broad molecular weight distribution was purchased from Aldrich to evaluate whether linear or star polymers with narrow molecular weight distributions exhibit superior rheological properties compared to those with broad distributions.

Rheology tests were performed using a 20% w/w polymer solution, including dioctyl adipate (DOA) plasticizer. The viscosity and shear stress of the sample solutions were measured at various shear rates at 25 °C. The entangled and randomly oriented polymer chains become dispersed during flow, reducing molecular interactions and creating more free space, decreasing viscosity in polymer solutions. The polymers were completely disentangled at elevated shear rates, resulting in the system's viscosity attaining the infinite shear viscosity plateau (η_∞). The commercially used linear PS mixture containing DOA exhibited completely shear rate-independent behavior because it contained polymer chains of different lengths with a broad molecular weight distribution. The star polymer exhibited a smaller hydrodynamic volume and radius of gyration, and thus lower viscosity, compared to its linear analogs of similar molar mass.

These findings demonstrate that polymer topology significantly influences rheological behavior, indicating that star-shaped architectures offer advantages for applications requiring lower viscosity and improved processability. Future research should investigate a broader range of functional star polymers, assess their performance under conditions relevant to industry, and clarify structure–property relationships to inform the design of materials with specific rheological characteristics.

Acknowledgments

We thank Prof. Dr. Aydan Dag for generously allocating the Schlenk Line used in this work.

Authors' Contributions

Author wrote the manuscript.

Competing Interests

The authors declare that they have no conflict of interest.

References

[1] J. M.Ren, T. G.McKenzie, Q.Fu, , E. H.Wong, J. Xu, Z.An, S. Shanmugam, T. P. Davis, C. Boyer, and G. G. Qiao, Star polymers, *Chemical Reviews*, *116* (12), 6743-6836, (2016).

[2] P. Tikhonov, N. Vasilenko, and A.Muzafarov, Multiarm star polymers. Fundamental aspects. A review, Doklady Chemistry: *Springer*, Vol. 496, pp 1-17,(2021).

[3] W.Wu, W. Wang, and J. Li, Star polymers: Advances in biomedical applications, *Progress in Polymer Science*, *46*, 55-85, (2015).

[4] J.Du, and Y. Chen, Preparation of poly (ethylene oxide) star polymers and poly (ethylene oxide)–polystyrene heteroarm star polymers by atom transfer radical polymerization, *Journal of Polymer Science Part A: Polymer Chemistry*, *42* (9), 2263-2271, (2004).

[5] A. Herberg, X Yu,. and D.Kuckling, End group stability of atom transfer radical polymerization (ATRP)-synthesized poly (N-isopropylacrylamide): Perspectives for diblock copolymer synthesis, *Polymers*, *11* (4), 678, (2019).

[6] J. Xia, X.Zhang, and K.Matyjaszewski, Synthesis of star-shaped polystyrene by atom transfer radical polymerization using an "arm first" approach, *Macromolecules*, *32* (13), 4482-4484, (1999).

[7] M. Spiniello, A. Blencowe, and G. G.Qiao, Synthesis and characterization of fluorescently labeled core cross-linked star polymers, *Journal of Polymer Science Part A: Polymer Chemistry*, *46* (7), 2422-2432, (2008).

[8] N. Cakir Yigit, G.Hizal, and U.Tunca, A powerful tool for preparing peripherally post-functionalized multiarm star block copolymer, *Polymer Bulletin*, *75*, 3523-3538, (2018).

[9] D. S. Esen, Cakir N.Yigit, U. Tunca, G. Hizal, and N.Arsu, Synthesis and characterization of multiarm (Benzoin-PS) m-polyDVB star polymer as a polymeric photoinitiator for polymerization of acrylates and methacrylates, *Journal of Polymer Science*, *59* (18), 2082-2093, (2021).

[10] Y. Dai, H. Sun, S. Pal, Y. Zhang, S.Park, C. P. Kabb, W. D. Wei, and B. S. Sumerlin, Near-IR-induced dissociation of thermally-sensitive star polymers, *Chemical Science*, *8* (3), 1815-1821, (2017).

[11] T. K. Goh, K. D. Coventry, A.Blencowe, and G. G. Qiao, Rheology of core cross-linked star polymers, *Polymer*, *49* (23), 5095-5104, (2008).

[12] D. Truzzolillo, D. Vlassopoulos, and M. Gauthier, Osmotic interactions, rheology, and arrested phase separation of

star–linear polymer mixtures, *Macromolecules*, *44* (12), 5043-5052, (2011).
[13] C. Wang, W. He, F. Wang, H.Yong, T. Bo, D. Yao, and M. Li, Recent progress of non-linear topological structure polymers: synthesis, and gene delivery. *Journal of Nanobiotechnology*, *22*(1), 40, (2024)
[14] F. Navaie, E.Esmaeilnezhad, and H.-J. Choi, Effect of rheological properties of polymer solution on polymer flooding characteristics, *Polymers*, *14* (24), 5555, (2022).
[15] L. Gury, M. Gauthier, M. Cloitre, and D. Vlassopoulos, Colloidal jamming in multiarm star polymer melts, *Macromolecules*, *52* (12), 4617-4623, (2019).
[16] T. Ebrahimi, S. G.Hatzikiriakos, and P. Mehrkhodavandi, Synthesis and Rheological Characterization of Star-Shaped and Linear Poly (hydroxybutyrate), *Macromolecules*, *48* (18), 6672-6681, (2015).
[17] F. Snijkers, H. Y. Cho, A. Nese, K. Matyjaszewski, W. Pyckhout-Hintzen, and D.Vlassopoulos, Effects of core microstructure on structure and dynamics of star polymer melts: from polymeric to colloidal response, *Macromolecules*, *47* (15), 5347-5356, (2014).
[18] A. Miros, D.Vlassopoulos, A. Likhtman, and J. Roovers, Linear rheology of multiarm star polymers diluted with short linear chains, *Journal of Rheology*, *47* (1), 163-176, (2003).
[19] P. Polanowski, K. Hałagan, and A.Sikorski, Star polymers vs. dendrimers: Studies of the synthesis based on computer simulations, *Polymers*, *14* (13), 2522, (2022).
[20] S. Liu, J. Zhang, L. R. Hutchings, L. Peng, X. Huang, and Q.Huang, The "solvent" effect of short arms on linear and nonlinear shear rheology of entangled asymmetric star polymers, *Polymer*, *281*, 126125, (2023).
[21] E. Van Ruymbeke, E. B. Muliawan, D.Vlassopoulos, H. Gao, and K.Matyjaszewski, Melt rheology of star polymers with large number of small arms, prepared by crosslinking poly (n-butyl acrylate) macromonomers via ATRP, *European Polymer Journal*, *47* (4), 746-751. (2011).
[22] J. M. Ren, T. G. McKenzie, Q. Fu, E. H. Wong, J. Xu, Z. An, and G. G. Qiao, Star polymers. *Chemical reviews*, *116*(12), 6743-6836. (2016).
[23] A.Mandal, and A. F. Kilbinger, Catalytic Living ROMP: Synthesis of Degradable Star Polymers. *ACS Macro Letters*, *12*(10), 1372-1378. (2023).
[24] K. Sparnacci, T. Frison, E. Podda, D. Antonioli, M. Laus, M. Notari, and R. Po, Core-crosslinked star copolymers as viscosity index improvers for lubricants. *ACS Applied Polymer Materials*, *4*(12), 8722-8730. (2022).
[25] Z. Luo, L. Wang, J. Pei, P. Yu, and B. Xia, A novel star-shaped copolymer as a rheology modifier in water-based drilling fluids, *Journal of Petroleum Science Engineering*, *168*, 98-106. (2018).
[26] G. Jian, , A. Santra, C. Mbuncha, and G. Ross, A novel star polymer for regulating fluid loss in oil-based mud under high temperature conditions, *Journal of Molecular Liquids*, *389*, 122815. (2023).
[27] N. Cakir Yigit, , G. Hızal, and U. Tunca, Synthesis of multiarm star block copolymer based on host-guest inclusion complexation, *Journal of innovative engineering and natural science (Online)*, *2* (1), 1-16. (2022).
[28] D. Srivastva, and A. Nikoubashman, (Flow behavior of chain and star polymers and their mixtures, *Polymers*, *10* (6), 599. (2018).
[29] P. Kratochvíl, and M. Netopilík, On the contraction factors of long-chain branched macromolecules, *European Polymer Journal*, *51*, 177-181. (2014).